

Mapping the Epitope of an Inhibitory Monoclonal Antibody to the C-terminal DNA-binding Domain of HIV-1 Integrase*

Received for publication, June 1, 2001, and in revised form, January 11, 2002
Published, JBC Papers in Press, January 22, 2002, DOI 10.1074/jbc.M105072200

Jizu Yi‡, Hong Cheng, Mark D. Andrade, Roland L. Dunbrack, Jr., Heinrich Roder§, and Anna Marie Skalka¶

From the Fox Chase Cancer Center, Institute for Cancer Research, Philadelphia, Pennsylvania 19111

Integrase (IN) catalyzes the insertion of retroviral DNA into chromosomal DNA of a host cell and is one of three virus-encoded enzymes that are required for replication. A library of monoclonal antibodies against human immunodeficiency virus type 1 (HIV-1) IN was raised and characterized in our laboratory. Among them, monoclonal antibody (mAb) 33 and mAb32 compete for binding to the C-terminal domain of the HIV-1 IN protein. Here, we show that mAb33 is a strong inhibitor of IN catalytic activity, whereas mAb32 is only weakly inhibitory. Furthermore, as the Fab fragment of mAb32 had no effect on IN activity, inhibition by this mAb may result solely from its bivalency. In contrast, Fab33 did inhibit IN catalytic activity, although bivalent binding by mAb33 may enhance the inhibition. Interaction with Fab33 also prevented DNA binding to the isolated C-terminal domain of IN. Results from size-exclusion chromatography, gel electrophoresis, and matrix-assisted laser desorption ionization time-of-flight mass spectrometric analyses revealed that multiple Fab33-IN C-terminal domain complexes exist in solution. Studies using heteronuclear NMR showed a steep decrease in ^1H - ^{15}N cross-peak intensity for 8 residues in the isolated C-terminal domain upon binding of Fab33, indicating that these residues become immobilized in the complex. Among them, Ala²³⁹ and Ile²⁵¹ are buried in the interior of the domain, whereas the remaining residues (Phe²²³, Arg²²⁴, Tyr²²⁶, Lys²⁴⁴, Ile²⁶⁷, and Ile²⁶⁸) form a contiguous, solvent-accessible patch on the surface of the protein likely including the epitope of Fab33. Molecular modeling of Fab33 followed by computer-assisted docking with the IN C-terminal domain suggested a structure for the antibody-antigen complex that is consistent with our experimental data and suggested a potential target for anti-AIDS drug design.

Integrase (IN)¹ is one of three virus-encoded enzymes that are required for retroviral replication (1). IN catalyzes insertion of the linear double-stranded viral DNA into the chromosomal DNA of a host cell. The IN protein comprises three distinct regions known as the N-terminal, catalytic core, and C-terminal domains (see Fig. 1A) (2, 3). The isolated N-terminal domain (residues 1 to ~50) assumes a three-helix bundle structure with a helix-turn-helix motif stabilized by Zn²⁺ coordination that stimulates enzymatic activity *in vitro* (4, 5). The N-terminal domain contributes to formation of tetrameric or higher multimeric forms of the protein (6–8). Crystallographic analysis of the catalytic core domains of human immunodeficiency virus type 1 (HIV-1) IN and avian sarcoma virus IN revealed that each subunit binds at least one divalent cation cofactor, Mg²⁺ or Mn²⁺, mediated by acidic residues in the highly conserved D,D(35)E motif that comprises the active site of the enzyme (9–12). Binding of the metal cofactor to this motif activates HIV-1 IN (13, 14) and stimulates preferential attachment of the protein to its viral DNA substrate (15). The C-terminal domain, comprising amino acids 220–270, binds DNA. Its NMR structure resembles that of the SH3 domain, a motif known to promote protein-protein interactions (16–18). Although the isolated C-terminal domain forms a homodimer in solution, only the catalytic core domain forms a dimer in the crystal structure of a two-domain derivative of HIV-1 IN that includes the core and C-terminal domains (19). In such crystals, the C-terminal domain moieties are separated from each other by 55 Å, but are involved in a variety of contacts with C-terminal domains in adjacent unit cells.

IN proteins must recognize and bind to both viral and host cell target DNAs. In the processing reaction, two nucleotides are removed from the 3'-ends of the viral DNA. These new 3'-ends are then joined to phosphorus atoms in the backbone of both strands of the target DNA in a concerted cleavage and ligation reaction. The strongest DNA-binding determinants of HIV-1 IN have been localized to the C-terminal domain, but such binding is sequence-independent. Despite intense efforts in many laboratories, the detailed mechanism by which IN interacts with host and viral DNAs remains unknown. To address this and other questions of structure and function, a library of monoclonal antibodies (mAbs) was raised against HIV-1 IN and characterized in our laboratory (20). Several of these mAbs inhibit the enzymatic activities of IN *in vitro*. Among these, mAb17 binds to the N-terminal domain, mAb4 binds to the catalytic core, and mAb32 and mAb33 bind to the C-terminal domain of IN (see Fig. 1A). Details of the binding of

* This work was supported by National Institutes of Health Grants AI40385, CA71515, and CA06927 and by an appropriation from the Commonwealth of Pennsylvania. The NMR Facility was supported by an endowment grant from the Kresge Foundation. The costs of publication of this article were defrayed in part by the payment of page charges. This article must therefore be hereby marked "advertisement" in accordance with 18 U.S.C. Section 1734 solely to indicate this fact.

‡ Present address: Dept. of Pathology, Mount Sinai School of Medicine, New York University, One Gustave Levy Place, New York, NY 10029.

§ To whom correspondence may be addressed: Fox Chase Cancer Center, Inst. for Cancer Research, 7701 Burholme Ave., Philadelphia, PA 19111. Tel.: 215-728-3123; Fax: 215-728-3574; E-mail: H_Roder@fcc.edu.

¶ To whom correspondence may be addressed: Fox Chase Cancer Center, Inst. for Cancer Research, 7701 Burholme Ave., Philadelphia, PA 19111. Tel.: 215-728-2490; Fax: 215-728-2778; E-mail: AM_Skalka@fcc.edu.

¹ The abbreviations used are: IN, integrase; HIV-1, human immunodeficiency virus type 1; mAb, monoclonal antibody; SPR, surface plasmon resonance; ELISA, enzyme-linked immunosorbent assay; HSQC, heteronuclear single-quantum correlation; MALDI-TOF, matrix-assisted laser desorption ionization time-of-flight.

the N-terminal domain to the inhibitory mAb17 have been reported (21); its epitope was mapped to a relatively neutral surface of the dimeric N-terminal domain, likely to be involved in protein-protein interaction. Here, we describe detailed binding studies and structural analyses of the interaction of the C-terminal domain-specific mAb33. We show that binding of Fab33 prevented the interactions of the C-terminal domain with DNA substrates and also inhibited the enzymatic activity of full-length IN, whereas binding of Fab32 produced neither effect. The epitope recognized by Fab33 was mapped to the three-dimensional structure of IN-(220–270) using heteronuclear NMR spectroscopy and computer-assisted molecular modeling.

EXPERIMENTAL PROCEDURES

HIV-1 IN Proteins and Anti-IN Monoclonal Antibodies—Construction of plasmid pET29b, encoding wild-type HIV-1 IN, IN-F185K/C280S, and IN-3CS (with three Cys → Ser substitutions at positions 56, 65, and 280), was reported previously (13–15). For NMR experiments, the protein expression vectors pET28b/IN-(220–270) and pET28b/IN-(220–288) were prepared by inserting sequences encoding amino acids 220–270 and 220–288 of HIV-1 IN, respectively, into plasmid pET28b (Novagen, Madison, WI) as described (21). The products include four expression plasmid-encoded amino acids (GSHM) at their N termini, which remain after thrombin cleavage to remove the His₆ tag. ¹⁵N-Labeled IN-(220–270) and ²H, ¹⁵N-labeled IN-(220–288) were purified from *Escherichia coli* strain BL21(DE3) grown in M9 minimal medium with [¹⁵N]ammonium chloride as the sole nitrogen source and in H₂O or 99% D₂O. As higher yield and better purification were obtained with IN-(220–288), this protein was used for NMR analysis of the mAb33 epitope. Procedures for protein expression and purification, monoclonal antibody preparation, and isolation of Fab fragments were reported previously (21, 22).

Oligonucleotide Activity Assay—The effect of mAb32 and mAb33 on the enzymatic activity of full-length HIV-1 IN was determined by measuring both the processing and joining reactions using a 21-base pair oligonucleotide duplex that represents the viral U5 DNA end as substrate (13). Assay conditions are described in the relevant figure legends.

Kinetic Analysis and Efficiency of IN Binding to DNA Substrates—Surface plasmon resonance (SPR; BIACORE) was employed to analyze the interactions between the isolated C-terminal domain of IN and DNA substrates. Double-stranded oligonucleotides representing either the viral U5 DNA end (20-mer) or a target DNA substrate (24-mer) with no sequence match with viral DNA ends were immobilized on the surface of a chip as described (15). To allow association, solutions of the IN protein were applied to a chip containing immobilized DNA. Dissociation of IN from the nucleoprotein complex was monitored in real-time after application of buffer to wash the chip. The kinetic rate constants for dissociation (k_{off} or k_d) and for apparent association (k_{on} or k_a) were obtained by fitting the real-time data, and the apparent dissociation constant was calculated as $K_d = k_{\text{off}}/k_{\text{on}}$ (15).

Enzyme-linked Immunosorbent Assay (ELISA)—The HIV-1 IN-3CS protein was immobilized on 96-well high binding microtiter plates by applying a solution containing 1 μg IN/well in a total volume of 50 μl of Tris-buffered saline (20 mM Tris-HCl (pH 7.5) and 150 mM NaCl). After overnight incubation, 50 μl of 1 mg/ml bovine serum albumin in the above buffer was added to each well, and the plates were incubated for 2 h to block the remaining binding sites. The plates were subsequently washed with 200 μl of Tris-buffered saline four times, followed by addition of primary antibodies and secondary antibodies labeled with horseradish peroxidase. The standard protocol was then followed, and the relative binding efficiency of monoclonal antibody to the immobilized IN protein was determined by measurement of absorbance at 405 nm (13, 20, 21).

NMR Spectroscopy—NMR spectra were recorded at 37 °C on a Bruker DMX 600-MHz spectrometer equipped with a 5-mm *x,y,z*-shielded pulsed-field gradient triple-resonance probe. Typically, each sample contained ~0.5 mM IN-(220–288) dissolved in 95% H₂O and 5% D₂O at a final buffer concentration of 50 mM NaH₂PO₄ (pH 6.5), 100 mM NaCl, and 0.5 mM EDTA, which was the same as that used by Lodi *et al.* (16). Protein-mAb interaction was studied by recording ¹H, ¹⁵N HSQC NMR spectra (23) for each sample of IN-(220–288) mixed with Fab33 at Fab/IN ratios of 0.16:1.0, 0.35:1.0, 0.55:1.0, 0.75:1.0, and 0.98:1.0. To minimize line broadening due to dipole-dipole coupling, the IN protein was uniformly labeled with ²H in addition to ¹⁵N (24). Each ¹H, ¹⁵N

HSQC spectrum was recorded as a 2048 (¹H) × 128 (¹⁵N) data matrix with acquisition times of 285 ms in *t*₂ and 78 ms in *t*₁. The data were acquired with 32 scans for each hypercomplex *t*₁/*t*₂ increment with an interscan delay of 1 s. The total acquisition time was 3.5 h for each spectrum. The NMR data were processed using XWINNMR2 (Bruker) and analyzed using Felix2000 NMR processing software (MSI). The ¹H, ¹⁵N HSQC spectrum of IN-(220–270) was assigned on the basis of the work of Lodi *et al.* (16) and Clore.² Thirty-nine well resolved peaks in the HSQC spectrum of IN-(220–288) were assigned by comparison. (The remaining resonances were obscured by the signals from the C-terminal tail (residues 271–288).) As a qualitative measure of the line broadening due to addition of Fab33, we determined peak heights for resolved cross-peaks in the base line-corrected HSQC spectra. Peak heights show a more linear dependence on the concentration ratio of Fab33 to IN-(220–288) than peak volumes. Solvent-accessible surface areas were calculated using GETAREA Version 1.1 (Sealy Center for Structural Biology, University of Texas Medical Branch, Galveston, TX) (25).

Mass Spectrometry—MALDI-TOF mass spectrometric analysis was carried out as described previously (21, 22). Slight modifications in experimental conditions are described in the relevant figure legends.

Size-exclusion Chromatography—The assay was performed on a Superdex 200/PC3.2 column (3.2 mm × 30 cm) equilibrated with 50 mM Hepes (pH 7.5) containing 300 mM NaCl. The column was calibrated with standard proteins of known molecular masses (Bio-Rad), thyroglobulin (670 kDa), γ-globulin (158 kDa), bovine serum albumin (68 kDa), ovalbumin (44 kDa), and myoglobin (17 kDa), using linear regression on a plot of log molecular mass *versus* elution time. Samples to be analyzed (each protein at 120 μM) were incubated for 30 min on ice prior to injection and eluted at 0.2 ml/min. The eluted proteins were monitored by measuring the absorbance at 280 or 220 nm for IN-(220–288).

Chemical Cross-linking—IN-(220–288) was mixed with Fab33 and incubated in the presence of 2.5 mM glutaraldehyde cross-linker in 20 mM Hepes (pH 7.5) and 500 mM NaCl for 30 min at 25 °C. Each protein was present at a final concentration of 28 μM in the 1:1 ratio reaction. Reactions were terminated by quenching with 40 mM glycine for 10 min prior to addition of loading buffer for analysis by SDS-PAGE. Equal samples of each reaction were loaded on a 16% Tris/glycine gel prior to visualization by silver staining.

Modeling of mAb33—Modeling of the Fv fragment of mAb33 was performed as described previously (21) using PSI-BLAST to compare the sequences of the heavy and light chain variable domains with sequences of known structures in the Protein Data Bank (codes 1IBG and 1A7O, respectively). Sequence identity was 49% for the heavy chain and 62% for the light chain. Side chain coordinates were predicted with the SCWRL program (26).

Docking Fab33 with IN-(220–270)—As described previously (21) the program HEX Version 2.3 (27)³ was used to identify a reasonable structure for the complex. The calculations were started in a conformation with the antibody combining site and residues of IN-(220–270) (Protein Data Bank code 1QMC, Ref. 18) identified as potential points of contact, pointed toward one another. The proteins were then allowed to move in a 60° arc (±30°) in each direction and ±8 Å along the intermolecular axis to produce the best fit. The solvent-accessible surface area buried upon Fab-IN complex formation is calculated as the difference between the accessible surface area of complexed IN-(220–270) and free IN-(220–270).

RESULTS

Binding Properties of mAb32 and mAb33—Our previous studies showed that the activity of HIV-1 IN is stimulated by preincubation with the divalent metal ion (Mg²⁺ or Mn²⁺) required for catalysis (13). Such stimulation is correlated with a conformational change that is blocked by the binding of mAb33 to the apoenzyme. mAb33 also inhibits the processing, joining, and disintegration activities of HIV-1 IN (14). Our previous analyses also showed that mAb33 and mAb32 compete for binding to the C-terminal region of the HIV-1 IN protein (20). Furthermore, the binding of Fab32 has been mapped to specific residues in the C-terminal domain based on MALDI-TOF mass spectrometric analysis combined with time-limited proteolysis (22). To further investigate the binding of

² G. M. Clore, personal communication.

³ Available at www.biochem.abdn.ac.uk.

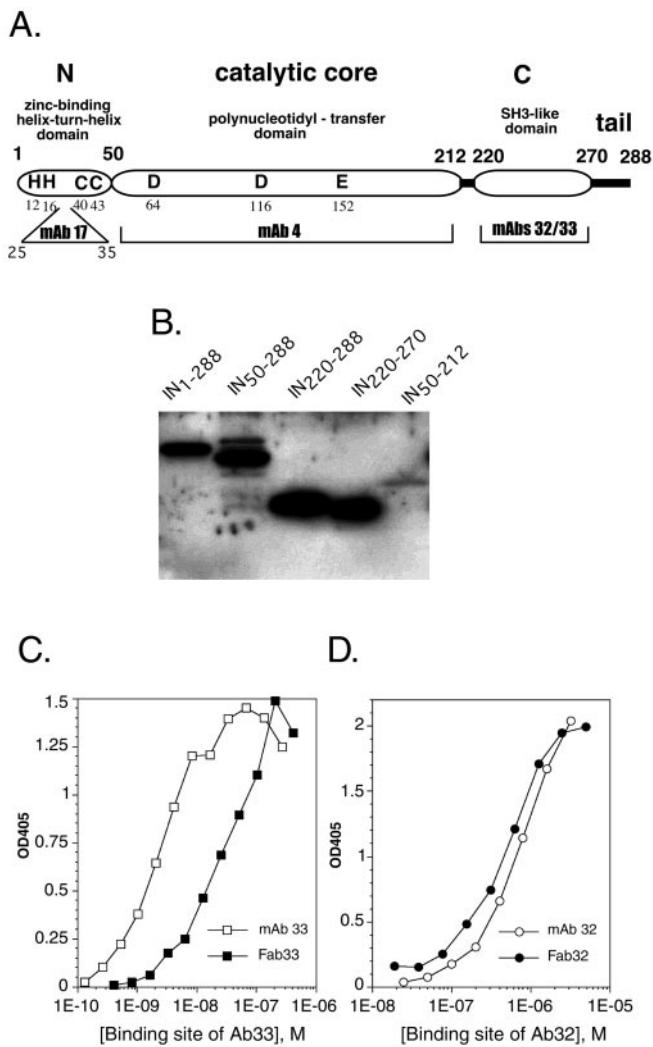


FIG. 1. Structural and functional domains of HIV-1 IN and their interactions with mAb33 and mAb32. A, a linear model of the HIV-1 integrase protein and its domains recognized by four mAbs. The N-terminal domain with a helix-turn-helix structure includes the conserved residues HHCC that bind Zn^{2+} . The catalytic core domain with polynucleotidyl transfer activity includes a highly conserved D,D(35)E motif and binds Mg^{2+} or Mn^{2+} . The C-terminal domain with an SH3-like structure has nonspecific DNA-binding activity. The numbers above the map indicate the approximate borders of domains, and numbers below the map show the positions of conserved residues of HIV-1 IN (2). mAb17, mAb4, and mAb33/32 recognize N-terminal, catalytic core, and C-terminal domains, respectively (20). B, immunoblot analysis with mAb33 and truncated HIV-1 IN proteins. The assay was performed as described previously (20). Proteins (1.2 μ g/lane) were subjected to electrophoresis on a 12% polyacrylamide gel (with SDS) and then transferred to a nitrocellulose membrane. mAb33 (1:2000 dilution or 0.04 μ g/ml) was added to test its recognition of the indicated truncated proteins as determined by chemiluminescence with a Pierce Supersignal CL-HRP substrate system. C, ELISA analyses showing mAb33 and Fab33 interaction with HIV-1 IN-3CS. A high binding microtiter plate was coated with full-length IN-3CS, blocked with bovine serum albumin, and treated as described under "Experimental Procedures." Either mAb33 (\square) or Fab33 (\blacksquare) was subsequently added as primary antibody, followed by a standard ELISA protocol using a secondary antibody against the κ -chain. D, ELISA analyses showing the interaction of mAb32 (\circ) and Fab32 (\bullet) with HIV-1 IN-3CS. The experimental conditions were as described for C.

mAb33, we first performed immunoblot analyses with full-length HIV-1 IN (residues 1–288) and four different truncated proteins: IN-(50–212) (the isolated catalytic core domain), IN-(50–288) (the catalytic core and C-terminal domains), IN-(220–270) (the C-terminal domain only), and IN-(220–288) (the C-terminal domain and the "tail") (Fig. 1B). The results show that

mAb33 bound only to fragments containing the C-terminal domain (amino acids 220–270) and that neither the C-terminal region of the core domain (IN-(50–212)) nor the tail of the C-terminal domain (IN-(271–288)) contributed significantly to recognition of mAb33, confirming and extending our previous observations (20). Thus, for further analysis of the mAb33-binding site, we used IN-(220–270) and the more soluble IN-(220–288) interchangeably.

To determine whether the effects on IN enzymatic activity are related to the ability of the bivalent antibodies to cross-link the protein, we compared the binding affinities and inhibitory activities of the intact antibodies (mAb32 and mAb33) with the corresponding Fab fragments (Fab32 and Fab33). ELISA studies revealed that mAb33 and Fab33 formed stable complexes with full-length HIV-1 IN-3CS, with half-saturation concentrations of 3.0×10^{-9} and 3.0×10^{-8} M, respectively (Fig. 1C). In contrast, there was no significant difference in the binding of mAb32 and Fab32 to HIV-1 IN-3CS; half-saturation concentrations were 5.0×10^{-7} and 4.0×10^{-7} M, respectively (Fig. 1D). However, these values are ~ 10 -fold higher than the dissociation constant determined for Fab33 and ~ 100 -fold higher than that of mAb33. Kinetic analysis using SPR showed that Fab33 formed a stable complex with IN-(220–270). The off-rate constant was $4.0 \times 10^{-3} s^{-1}$; the on-rate constant was $5.0 \times 10^5 s^{-1} M^{-1}$; and the dissociation constant (K_d) was ~ 8 nM. These data are consistent with results from ELISAs shown in Fig. 1C.

Inhibition of HIV-1 IN Activity—The effects of the mAbs and Fab fragments on HIV-1 IN processing activity were tested by quantitation of the -2 cleavage (processing) product from a 21-base pair oligodeoxynucleotide duplex that represents the viral U5 DNA end. The results show that both mAb33 and Fab33 inhibited HIV-1 IN processing (Fig. 2A) and joining (data not shown) activities. The half-inhibition concentrations (IC_{50}) of mAb33 and Fab33 were 0.18 and 1.8 μ M, respectively. The observation that mAb33 exhibited ~ 10 -fold higher inhibitory activity than its Fab fragment is consistent with the difference observed in the binding affinities of mAb33 and Fab33 (Fig. 1C). We conclude that bivalent binding is not required for inhibition by mAb33, but may enhance the inhibitory effect. These results are consistent with our previous observations that intracellular expression of the single-chain variable region of this antibody (single-chain Fv33) in a target cell prevents HIV-1 infection (28). Thus, the *in vivo* activity of single-chain Fv33 is correlated with the ability of Fab33 to inhibit IN enzymatic activity *in vitro*. On the other hand, mAb32 had a weak inhibitory effect ($IC_{50} \sim 2.0 \mu$ M), and Fab32 had no detectable effect on the processing activity of IN (Fig. 2A), although the binding affinities of these two reagents for IN were approximately equal (Fig. 1C). Thus, the inhibitory activity probably reflects the ability of the bivalent mAb32 to hold two IN molecules together in a nonproductive complex.

mAb33 Blocks DNA Binding to IN—Binding of the isolated catalytic core domain of HIV-1 IN to duplex oligodeoxynucleotide DNA substrates was not detectable in our previous studies using SPR (15). In contrast, the quantitative analysis shown in Fig. 2B indicated a dissociation constant (K_d) of 1.5 μ M for a duplex oligodeoxynucleotide representing the viral U5 DNA end in complex with the isolated C-terminal fragment IN-(220–288). The same K_d value was observed with IN-(220–270) (data not shown). These results indicated that as with mAb33 binding (Fig. 1B), the C-terminal 18-amino acid tail (amino acids 271–288) made no significant contribution to the stability of the DNA-IN-(220–288) complex. Furthermore, when a nonviral DNA substrate was immobilized, the K_d value measured was 1.7 μ M, confirming that DNA sequence does not

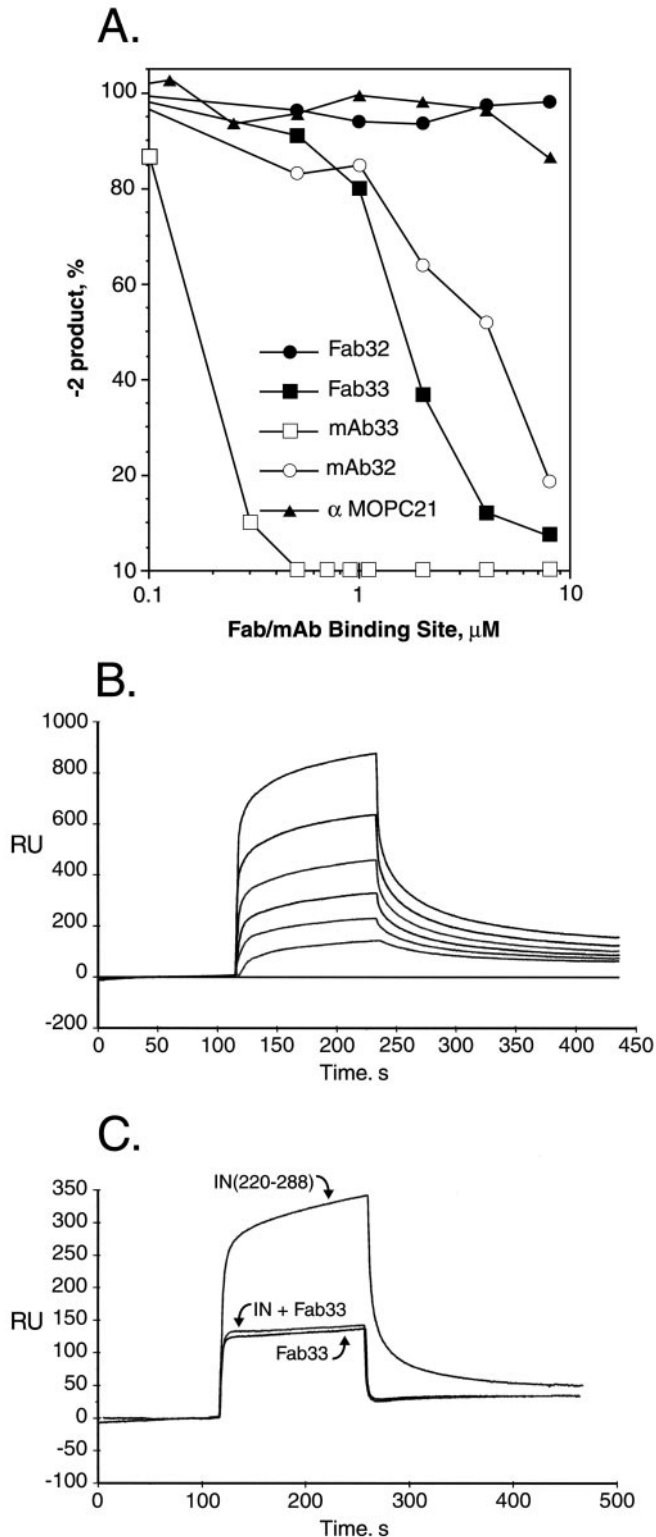


FIG. 2. Effects of mAb33 and mAb32 on HIV-1 IN action. *A*, effects of mAbs on the processing activity of HIV-1 IN. The wild-type HIV-1 IN protein ($1 \mu\text{M}$) was incubated at room temperature for 30 min with mAb32 (\circ), Fab32 (\bullet), mAb33 (\square), Fab33 (\blacksquare), or a control mouse IgG1 anti-MOPC21 mAb (\blacktriangle) in 15 mM Hepes (pH 7.5) containing 10 mM MnCl_2 , 6.67% Me_2SO , and 10% glycerol. The reaction was initiated by addition of $1 \mu\text{M}$ ^{32}P -labeled 21-bp model viral DNA substrate, and incubation was carried out for 30 min. Processing activity was measured by quantitation of the -2 cleavage product after exposure of the radioactive gel to an imaging plate and analysis on a Fuji MacBAS2000 imaging system (13). *B*, overlay plot of IN-(220–288) binding to a model viral DNA substrate. To an immobilized (180 relative response/resonance units (RU)) viral DNA substrate (21-mer), $60 \mu\text{l}$ of increasing

TABLE I
Effects of mAb33 and mAb32 on binding of IN-(220–288) to DNA substrates

Data were obtained from experiments similar to those described for Fig. 2C. After incubation in either the absence or presence of equimolar concentrations of mAb or Fab, IN-(220–288) was injected on the chip surface containing immobilized viral U5 model DNA substrate or model target DNA substrate. The response units (RU) were read after protein injection (15).

Antibody	Relative RU	DNA binding
	%	
Model viral DNA		
None	100	+
Anti-MOPC21	98 ± 3	+
Fab33	0.2 ± 1.0	–
Fab32	194 ± 10	+
Model target DNA		
None	100	+
Anti-MOPC21	101 ± 5.0	+
Fab33	0.0 ± 1.0	–
Fab32	121 ± 8	+

affect the affinity of the C-terminal domain interactions with DNA (29–31).

As both mAb33 and mAb32 bind to the C-terminal domain of HIV-1 IN, we investigated whether these mAbs could affect the ability of IN to bind to DNA substrates. Results of SPR measurements indicated that binding of the C-terminal domain to an immobilized DNA substrate was inhibited by preincubation of the protein with Fab33 (Fig. 2C); the binding profile for Fab33 + IN-(220–288) was indistinguishable from that of Fab33 alone. Detailed studies at various Fab33 concentrations indicated that this inhibition increased with increasing Fab33/IN ratio (data not shown). Complete inhibition was achieved at a Fab/IN-(220–288) ratio of 1:1 (as illustrated in Fig. 2C) or higher (data not shown). However, if IN-(220–288) was preincubated with equimolar amounts of Fab32, we observed an increase in the signal (Table I). No such increase was observed upon preincubation of IN-(220–288) with a nonspecific mAb (mouse anti-MOPC21). The relative response/resonance unit increase observed in the presence of Fab32 can be explained by the higher molecular mass of the Fab32-IN-(220–288) complex compared with IN-(220–288) alone. These results suggest that the Fab32-IN-(220–288) complex can bind to the immobilized DNA substrate, whereas binding of Fab33 to the C-terminal domain of IN inhibits the protein-DNA interaction.

mAb33 Binding Increases the Solubility of HIV-1 IN—The full-length HIV-1 IN protein is not soluble in low ionic strength buffer (21), even in the presence of a carrier protein such as bovine serum albumin (data not shown). As shown in Fig. 3, in the presence of a nonspecific control mouse monoclonal antibody (anti-MOPC21), full-length IN-3CS remained mainly in the pellet fraction after incubation in 15 mM Hepes (pH 7.5) and 50 mM NaCl (lane 4); quantitative analysis indicated that only 5% of IN-3CS remained in the supernatant (lane 3). However, 34 and 20% of IN-3CS were found in the supernatant fractions (Fig. 3, lanes 6, 7, 9, and 10) in the presence of mAb33 and mAb32, respectively. When Fab33 was present (Fig. 3, lanes 12 and 13), most of the IN-3CS ($\sim 93\%$) was soluble under the same conditions. Fab32 gave a similar effect as Fab33 (data not shown). These observations suggest that binding of these C

concentrations of IN protein (0.07 – $7.7 \mu\text{M}$) in buffer A (10 mM Hepes containing 200 mM NaCl and 0.05% Nonidet P-20) was injected at a flow rate of $30 \mu\text{l}/\text{min}$ and 25°C . *C*, Fab33 prevents DNA binding of IN-(220–288). IN-(220–288) alone, Fab33 alone, or IN-(220–288) after incubation with Fab33 in buffer A (IN + Fab33) was exposed to a model viral DNA substrate immobilized on the chip. Experimental conditions were as described for *B*.

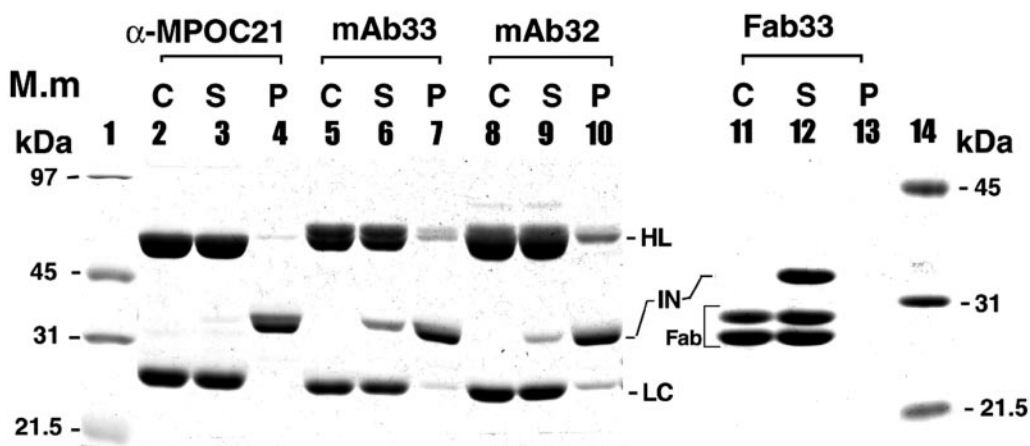


FIG. 3. **mAbs enhance HIV-1 IN solubility in low ionic strength buffer.** HIV-1 IN-3CS (6.6 μg) and anti-MPOC21 mAb (15 μg) (lanes 3 and 4), mAb33 (15 μg) (lanes 6 and 7), mAb32 (lanes 9 and 10), or Fab33 (10 μg) (lanes 12 and 13) were incubated in 30 μl of 10 mM Hepes (pH 7.5) containing 50 mM NaCl and 5% glycerol at room temperature for 15 min. The mixtures were then subjected to centrifugation at $17,000 \times g$ for 10 min. Supernatants (S) were separated from pellets (P). The protein distribution was analyzed by SDS-PAGE electrophoresis, followed by quantitation with Quantity One computer software (Bio-Rad). C indicates a control in the absence of IN (lanes 2, 5, and 11), and molecular mass markers are in lanes 1 and 14. The positions of IN, the heavy (HC) and light (LC) chains of mAbs, and the Fab33 fragments (Fab) are indicated.

terminus-specific antibodies increases the solubility of full-length HIV-1 IN.

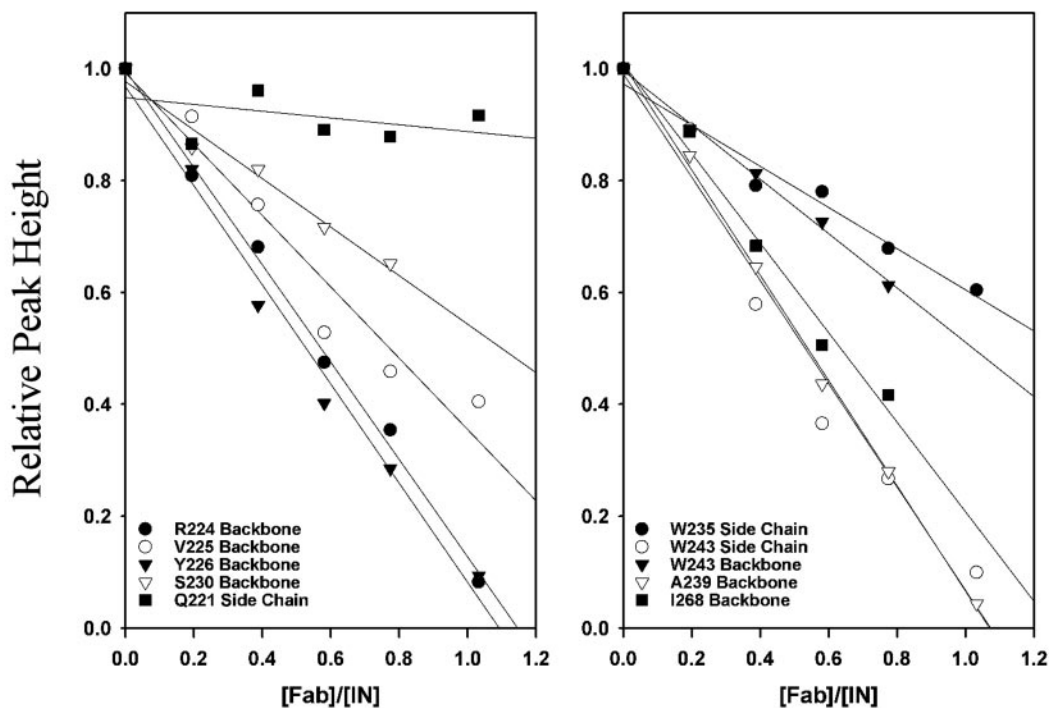
Identification of Fab33-binding Residues in IN—NMR analysis was carried out to identify residues in the C-terminal domain that are recognized by Fab33. IN-(220–288) labeled with ^2H and ^{15}N was mixed with increasing amounts of Fab33 to “titrate” the binding site on IN, and HSQC spectra were recorded as described under “Experimental Procedures.” The backbone amide ^1H and ^{15}N chemical shifts for 39 of 51 residues in the structured region of IN-(220–288) can be assigned by comparison with published assignments for free IN-(220–270) (16, 17). Addition of Fab33 resulted in a major decrease in peak intensity for most cross-peaks, but negligible changes in peak position, indicating that the dynamics of binding/dissociation between IN and Fab33 are slow on the NMR time scale, as expected from the low K_d and dissociation rate constant of the complex ($\sim 3.0 \times 10^{-8}$ M and 4.0×10^{-3} s $^{-1}$, respectively). The signals from nuclei in rigid parts of the bound IN domain are expected to be very weak because of the relatively large size of the Fab33-IN complex (~ 54 kDa for a 1:1 complex or ~ 110 kDa if two molecules of Fab33 bind per IN domain dimer; see below), resulting in severe line broadening. Indeed, the number of cross-peaks observed in the HSQC spectrum of IN-(220–288) was greatly reduced in the presence of equimolar Fab33. The remaining peaks can be attributed to mobile regions of the IN domain such as the C-terminal tail (residues 271–288) and exposed loops. When a small single-domain protein binds to a large antibody such as a Fab fragment (~ 47 kDa), it is possible that some residues in the protein still possess substantial mobility even in the presence of Fab, so the line broadening need not be a global effect over the entire NMR spectrum. Cheetham *et al.* (32) showed that even for a 28-residue peptide, some cross-peaks from the peptide were still detectable upon Fab binding in double-quantum filtered COSY spectra. Thus, we identified the residues involved in the epitope of the C-terminal domain of HIV-1 IN upon Fab33 binding by quantitative analysis of the decay in peak height for each resolved peak upon “titration” of the protein with Fab33.

In Fig. 4A, the relative peak heights of representative resolved cross-peaks in the HSQC spectra are plotted as a function of the [Fab33]/[IN-(220–288)] ratio. The slopes obtained by fitting the observed linear decrease in peak height for each resolved residue are shown in Fig. 4B. Eight residues (Phe²²³, Arg²²⁴, Tyr²²⁶, Ala²³⁹, Lys²⁴⁴, Ile²⁵¹, Ile²⁶⁷, and Ile²⁶⁸) exhibit

steep decays, with slopes >0.75 for each residue. As illustrated in Fig. 4A, the lines for these residues intercept the x axis near [Fab33]/[IN-(220–288)] = 1, suggesting a stoichiometry of one Fab molecule/one IN monomer and/or two Fab molecules/one IN dimer, *i.e.* 1:1 and 2:2 complexes, respectively. The normalized intensity of these peaks approximates the residual population of unbound IN-(220–288), indicating that the corresponding cross-peaks in the bound form are either shifted to other regions of the spectrum or are undetectable due to the increase in line width in the complex. Two of the 8 residues with slopes >0.75 (Ala²³⁹ and Ile²⁵¹) are buried in the hydrophobic core of the IN domain and are thus unlikely to be involved directly in antibody binding. The side chain of Trp²⁴³ (but not its backbone amide) also shows a slope >0.75 (Fig. 4A, right panel), but this residue is in the interface of the NMR dimer (Fig. 5) (16–18). However, the side chains of all other residues in this group (Phe²²³, Arg²²⁴, Tyr²²⁶, Lys²⁴⁴, Ile²⁶⁷, and Ile²⁶⁸) are at least partially exposed to the solvent in the NMR dimer. The steep decay in cross-peak intensity observed for these residues is likely due to their immobilization upon binding of Fab33. Inspection of the structure of the isolated IN-(220–270) domain shows that Phe²²³, Arg²²⁴, Tyr²²⁶, Ile²⁶⁷, and Ile²⁶⁸ lie on the solvent-exposed face of the domain comprising strands 1 and 5, whereas Lys²⁴⁴ is in a surface location extending from the dimer interface (Fig. 5) toward the Fab33 epitope. These 6 residues form a contiguous patch on the surface of the protein with a solvent-accessible area of ~ 650 Å².

Other residues experience a more gradual decrease in peak height (Fig. 4, A and B), which can be attributed to varying degrees of local mobility. Slopes <0.3 were observed for some side chain NH groups (*e.g.* Gln²²¹) (Fig. 4A). In addition, slopes of approximately 0.5 or less were observed for backbone amides of some surface-exposed residues in loop regions (Ser²³⁰, Gly²⁴⁷, and Ser²⁵⁵), as well as several unassigned peaks that we tentatively attribute to the C-terminal tail (residues 271–288; results not shown), all of which are expected to retain some degree of local mobility even in the presence of Fab33. However, inspection of the NMR structures of IN-(220–270) shows that 3 residues whose backbone amide slopes are <0.5 (Trp²⁴³, Val²⁵⁰, and Val²⁵⁹) are buried at the dimer interface (Fig. 5B). These residues are at the center of the tightly packed hydrophobic core of the dimeric structure and are unlikely to be mobile, unless the contact between IN monomers is perturbed by binding of Fab33. These results suggest that binding of

A



B

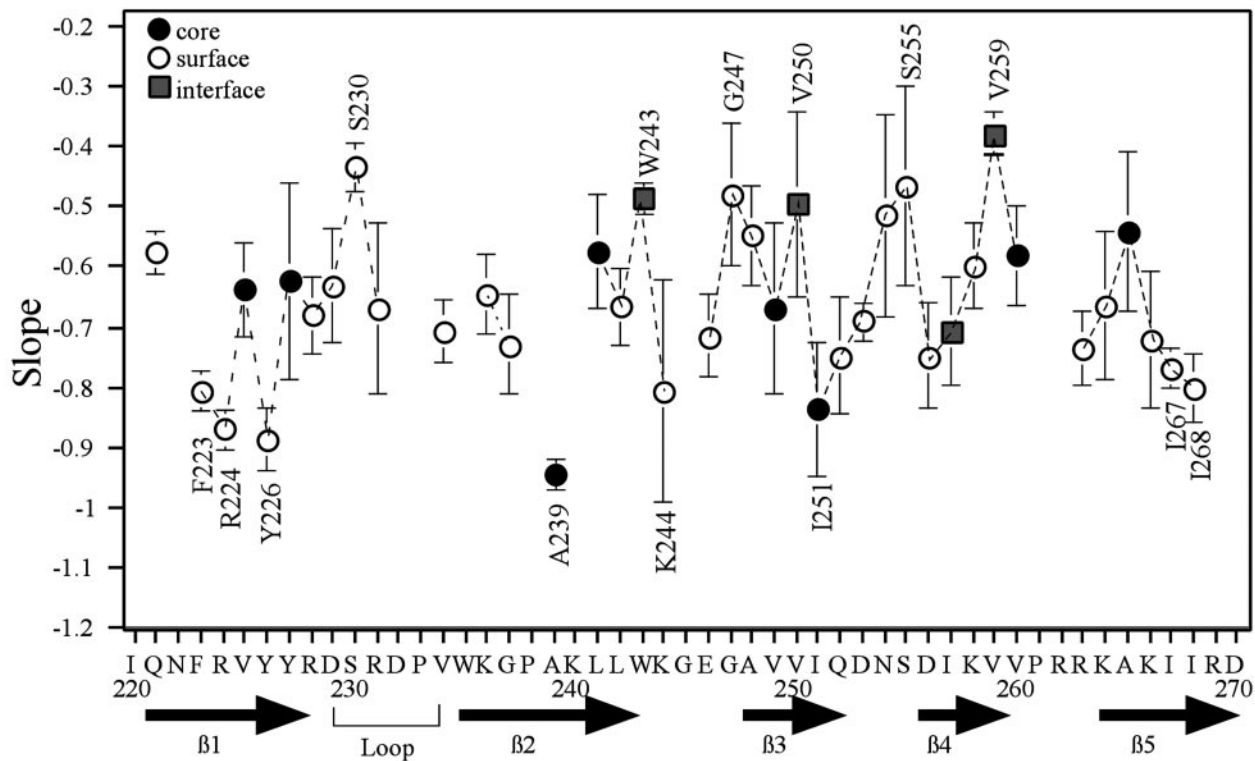


FIG. 4. **Epitope mapping by NMR.** A, relative peak heights (ratio of peak heights of Fab-bound IN-(220–288) divided by free IN-(220–288)) for representative ^1H - ^{15}N cross-peaks in the HSQC spectra of IN-(220–288) as a function of the concentration ratio of Fab33 to IN-(220–288). B, slopes obtained by linear regression of the Fab33-induced decay of peak amide NH contour heights (see A) versus residue number. Buried residues (<15% solvent-accessible surface area) are indicated by closed circles, surface residues by open circles, and residues buried at the monomer-monomer interface of the dimer structure of IN-(220–270) in solution (16–18) by shaded squares. The vertical lines indicate the S.E. calculated during linear regression. Dashed lines connect adjacent residues.

Fab33 either changes the local conformation of IN in the dimer interface region or promotes the dissociation of the dimer.

The C-terminal Domain Maintains a Monomer-Dimer Equi-

librium in Its Complex with Fab33—It has been reported that the C-terminal domain contributes to IN protein-protein interactions that produce the oligomeric form required for DNA

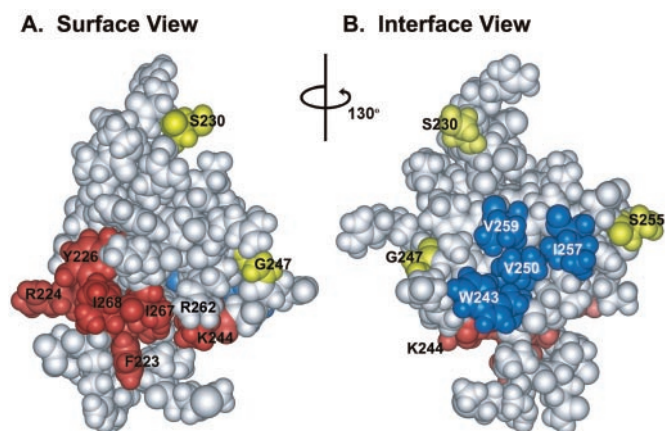


FIG. 5. **IN-(220–270) residues affected by binding of Fab33.** Shown is a space-filling model of a subunit of IN-(220–270) based on the NMR structure (Protein Data Bank code 1QMC) (18). Two views opposing (A) and facing (B) the dimer interface are shown. Immobilized residues (Fab33-induced decay rates >0.75) are shown in red; relatively mobile residues (slopes <0.5) are shown in yellow; and residues at the dimer interface are shown in blue.

integration (33, 34). The isolated C-terminal domain exists as a specific homodimer at concentrations of ~ 1 mM (16–18). Mass spectrometric analysis at a lower concentration (~ 1 μ M) indicated that both IN-(220–270) and IN-(220–288) were present as monomers and dimers (Fig. 6, A and B). To test whether these monomers and dimers reach a dynamic equilibrium, we analyzed a mixture of IN-(220–270) and IN-(220–288) by mass spectrometry. The results revealed that in addition to two homodimers of IN-(220–270) and IN-(220–288), a heterodimeric species, IN-(220–270)·IN-(220–288), was present (Fig. 6C). Thus, we conclude that a dynamic monomer-dimer equilibrium exists among molecules of the isolated C-terminal domain under these conditions.

To examine the composition of Fab33-IN complexes present in solution, we performed three types of analyses. In the first, Fab33/IN mixtures were subjected to mass spectrometric analysis as described above. Two additional peaks were detected in this analysis, with masses expected for 1:1 and 1:2 complexes of Fab33 and IN-(220–270) (Fig. 7A). Under the same conditions, no such complexes were observed between a non-cognate Fab (Fab17; Fig. 1) and IN-(220–270) (Fig. 7B), nor were complexes formed between Fab33 and a non-cognate antigen of similar size and pI (trypsin inhibitor, mass = 6517 Da; data not shown.) Due to the difficulty in resolving high molecular mass complexes by this method, a 2:2 species, if present, is unlikely to be detected. However, these results indicate that Fab33 can bind to both monomers and dimers of the C-terminal domain.

The composition of Fab33-IN-(220–288) complexes was next examined by SDS-PAGE analysis after cross-linking with glutaraldehyde (Fig. 8A). No bands were observed at the position expected for such complexes if either component was omitted (Fig. 8A, lanes 1 and 7, respectively), and no Fab33-IN-(220–288) complexes were observed in the absence of the cross-linker (lane 2). In the presence of cross-linker, IN-(220–288) alone formed large aggregates that migrated only to the edge of the stacking gel (Fig. 8A, lane 7). Under these experimental conditions, we expect that only a small fraction of the Fab33-IN-(220–288) complexes formed in the mixtures will be linked covalently (especially species that require multiple cross-links for detection on a denaturing gel). Nevertheless, the results showed that both the 1:1 and 1:2 complexes persisted when increasing concentrations of Fab33 were present; in fact, the complexes were detected most clearly at the higher Fab ratios (Fig. 8A, lanes 3–6). Thus, results from these cross-linking analyses indicate

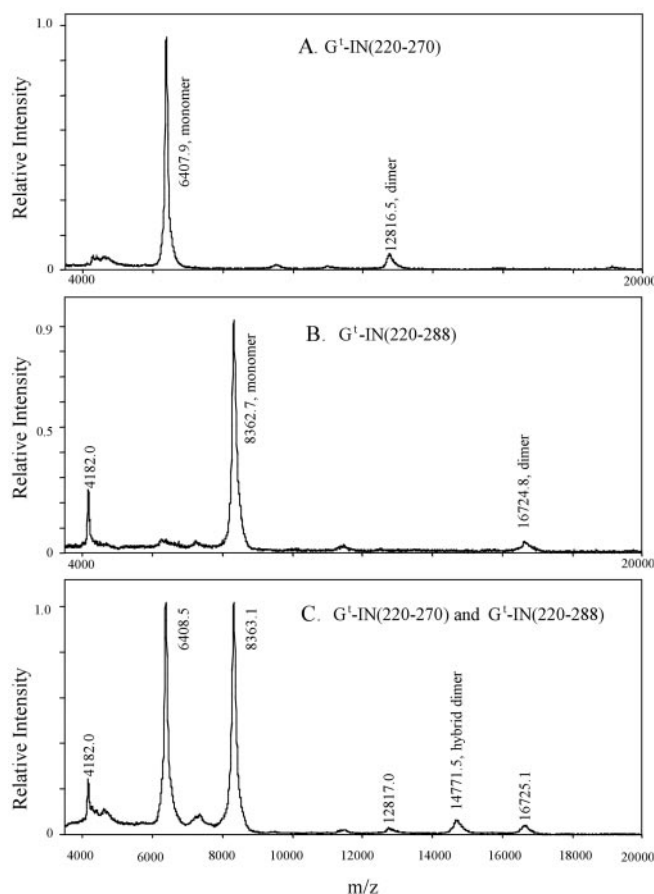


FIG. 6. **MALDI-TOF mass spectra of the C-terminal domains.** A, mass spectrometry of IN-(220–270). The prefix G^1 denotes the four expression plasmid-derived amino acids (GSHM) fused to the N termini of the C-terminal domain peptides, which contribute to the mass determinations. 0.4 μ l of 1 μ M G^1 -IN-(220–270) in 10 mM Hepes (pH 7.5) with 150 mM NaCl was placed on a target plate, followed by addition of 0.4 μ l of α -cyano-4-hydroxycinnamic acid. The mass spectrum was recorded using a VoyagerTM MALDI-TOF BioSpectrometer with accelerating voltage of $25,000$ V (21). B, mass spectrometry of G^1 -IN-(220–288). The experiment was carried out as described for A. C, mass spectrometry of a mixture of G^1 -IN-(220–270) and G^1 -IN-(220–288). 1 μ M G^1 -IN-(220–270) and 1 μ M G^1 -IN-(220–288) were mixed and incubated for 60 min at room temperature in 100 mM Hepes (pH 7.5) and 150 mM NaCl. The peaks at 4182 in B and C represent doubly charged monomers. The mixture was analyzed as described for A.

that Fab33 binding does not abrogate IN C-terminal domain multimerization.

As a final method to examine their composition, the Fab33-IN-(220–288) complexes were subjected to size-exclusion chromatography (Fig. 8B). In this analysis, the complex(es) eluted at a position consistent with an apparent molecular mass of 80 kDa. This value falls between that expected for 1:1 (55 kDa) and 2:2 (110 kDa) species and could represent the average mobility of multiple complexes in dynamic equilibrium during migration through the column. Fig. 6 provides evidence for such an equilibrium among IN C-terminal domain monomers. In addition to a mixture of 1:1 and 1:2 species, complexes comprising one Fab molecule and an IN-(220–288) oligomer would also be eluted at this position. In any case, elution earlier than the molecular mass standard of 68 kDa indicates that the Fab33-IN complex contains a multimer of IN-(220–288). Taken together, these three methods of analysis show that several Fab-IN complexes exist in solution and that Fab33 binding has no detectable effect on the multimerization of the C-terminal domain.

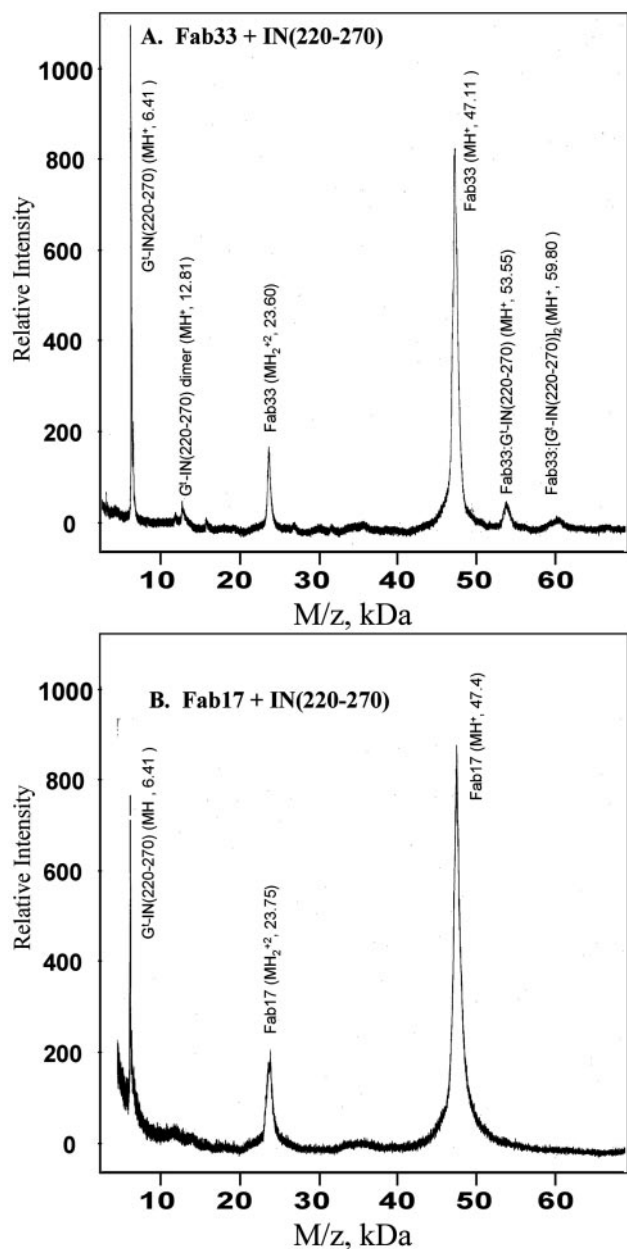


FIG. 7. Mass spectrometry of the Fab33-IN-(220-270) complex. Prefix G^+ is defined in Fig. 6. $2 \mu\text{M}$ G^+ -IN-(220-270) and $2 \mu\text{M}$ Fab33 (A) or Fab17 (B) were incubated in 5 mM Hepes (pH 7.5) with 50 mM NaCl for 30 min at room temperature. A $0.4\text{-}\mu\text{l}$ sample was mixed with $0.4 \mu\text{l}$ of sinapinic acid on a target plate and air-dried before the plate was inserted into the VoyagerTM MALDI-TOF BioSpectrometer. The spectrum was recorded as described in the legend to Fig. 6. The peaks at 47.11 and 23.60 kDa correspond to the singly and doubly charged Fab fragments, respectively. The peaks at 53.55 and 59.80 kDa were assigned as 1:1 (one Fab molecule/one G^+ -IN-(220-270) monomer (MH^+)) and 1:2 (one Fab molecule/one G^+ -IN-(220-270) dimer (MH^+)) complexes, respectively.

Modeling of Fab33 Bound to the C-terminal Domain of IN—Using the sequence determined for the Fab33 heavy and light chain complementarity-determining region (28) and the structure of homologous antibodies in the Protein Data Bank, a molecular model of Fab33 was constructed and then docked with the NMR structure of IN-(220-270) (18) as described under “Experimental Procedures.” The best model was obtained by starting docking after Fab33 was positioned close to the experimentally determined residues of the Fab33 epitope on IN-(220-270). Docking initiated at other positions either did

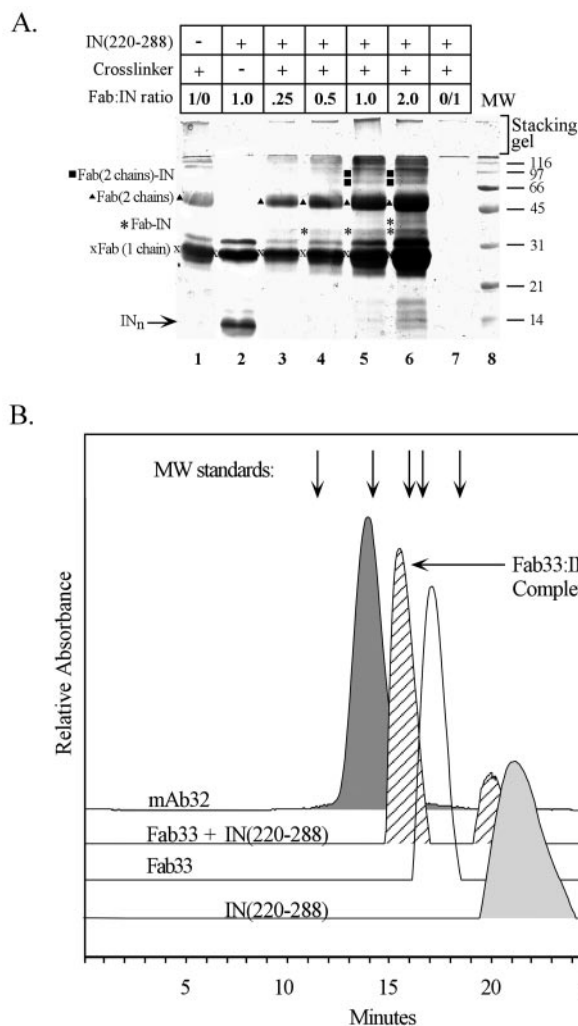


FIG. 8. Analysis of Fab-IN-(220-288) complexes. A, chemical cross-linking. Mixtures of Fab33 and IN-(220-288) were subjected to glutaraldehyde cross-linking as described under “Experimental Procedures” at the increasing Fab/IN ratios noted above each lane and then analyzed on a 16% reducing gel. \times , positions of Fab33 single chains; \blacktriangle , positions of cross-linked chains of Fab33; \rightarrow , position of uncomplexed IN-(220-288); * and \blacksquare , positions of cross-linked complexes of Fab33 (one and two chains, respectively) and IN-(220-288) (in each case, the position of the upper band is consistent with a size expected for a complex containing two IN-(220-288) molecules). The reaction for lane 2 contained no cross-linker; samples from reactions that contained only one component in the presence of cross-linker are shown in lanes 1 and 7. Migration positions of protein markers are shown in lane 8, and their molecular masses are indicated on the right in kilodaltons. B, size-exclusion chromatography of Fab-IN complexes. $\sim 10 \mu\text{l}$ of protein sample (1 mg/ml) was injected into a pre-equilibrated column and eluted as described under “Experimental Procedures.” The column was characterized with standard globular protein markers whose positions are indicated by arrows above the figure (left to right, 670, 158, 68, 44, and 17 kDa). The apparent molecular masses of mAb32 and Fab33 are consistent with known mass spectrometry-determined masses. The broad peak of IN-(220-288) likely reflects association and dissociation of multimers, which eluted slightly sooner in the mixture with Fab33 due to some partial association with Fab early in the run, prior to migrating independently.

not converge on a solution or did not produce a better fit. In the model, epitope residues are neatly bound by the complementarity-determining region loops of the antibody, with each loop contributing some residues to the complex (Fig. 9B). The surfaces are complementary in shape (Fig. 9A), with no large gaps between IN and the antibody. As this is a rigid model docking procedure, this model represents initial complementarity at the interface; further changes in side chain conformation of

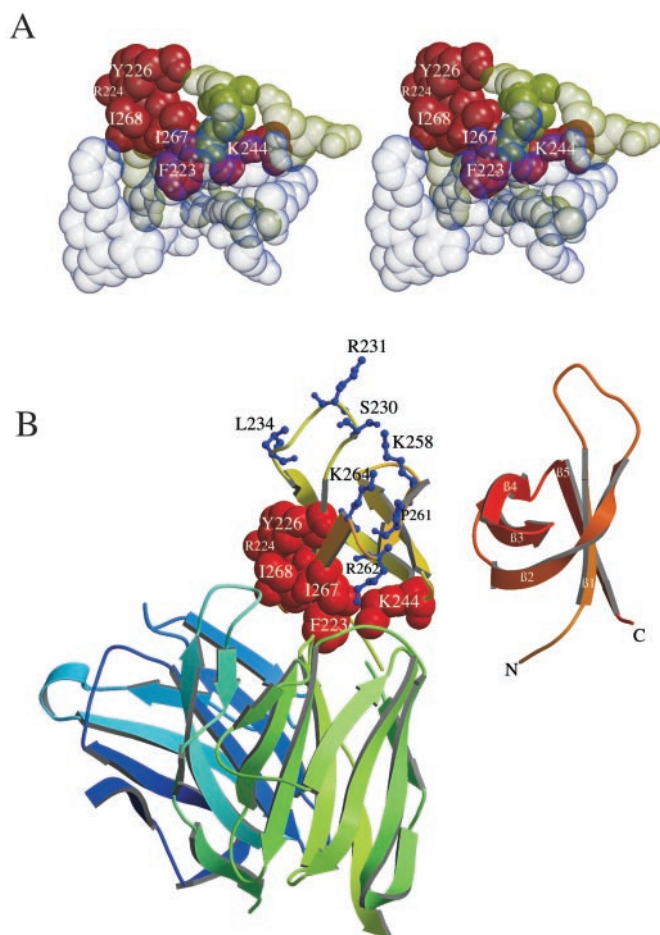


FIG. 9. Model of Fab33 binding to the C-terminal domain of IN. Using amino acids predicted for the sequence of Fab33, a model was produced and docked with the NMR structure of IN-(220–270) (Protein Data Bank code 1QMC) as described under “Results.” *A*, stereo diagram of the residues participating in this model interface. Fab33 residues within 5 Å of any IN residues are shown in *transparent blue*. IN residues determined by the NMR data to be a part of the Fab33 epitope are found in the core of this model interface colored in *red* and labeled with the one-letter amino acid code and IN residue number. Other IN residues that are also found within 5 Å of Fab33 atoms are portrayed in *transparent green* (Met²¹⁹, Gln²²¹, Asn²²², Gly²⁴⁵, Glu²⁴⁶, Gly²⁴⁷, Arg²⁶², Arg²⁶³, and Arg²⁶⁹). The total buried solvent-accessible surface area predicted in this model is 994 Å². The orientation of the interface portrayed is the same as shown in *B*. *B*, ribbon diagram of the model complex between Fab33 and IN-(220–270). IN residues in *red* are as described for *A*. IN residues thought to be important for DNA-binding activity (18, 34) are shown in *blue* ball-and-stick representation at the top of the left IN monomer. The β -strands of the Fab33 light and heavy chains are shown in *green* and *blue*, respectively. The IN-(220–270) domain on the right is the other half of a C-terminal domain dimer represented in a ribbon diagram. Molscript (Version 2.1.2) (38) and Raster3D (Version 2.5d) (39) were used to produce this figure.

both the IN epitope and Fab33 would be expected upon actual binding.

The residues with the steepest antibody-induced resonance intensities are all located at or near the binding interface predicted by the model. Another IN residue in this site is Arg²⁶². The Arg²⁶² cross-peak is obscured by other cross-peaks in the crowded region of the HSQC spectrum containing residues of the disordered tail (amino acids 271–288). As with the unambiguously assigned cross-peaks already listed as part of the Fab33 epitope, the tentative assignment of the Arg²⁶² cross-peak shows a steep drop in relative intensity (slope of -0.78). The solution structure of IN-(220–270) places Arg²⁶² adjacent to Lys²⁴⁴, with both residues positioned to directly interact with Fab33 in the model shown (Fig. 9). The buried

surface area of the 1:1 complex found in this model is calculated to be 994 Å², consistent with the high affinity interaction of Fab33 with IN-(220–270) we reported here. As illustrated in Fig. 9*B*, Fab33 binding is unlikely to affect several residues implicated in DNA binding (Ser²³⁰, Arg²³¹, Leu²³⁴, Lys²⁵⁸, Pro²⁶¹, and Lys²⁶⁴) either in the saddle formed by loops from each monomer or along the outer edge of each monomer (18). Although the antibody contacts some residues close to the dimer interface, it is not apparent in the model that binding of Fab33 should interfere with IN-(220–270) dimerization. The model suggests that two Fab molecules can bind simultaneously to one IN dimer without significant steric problems. Thus, the modeled complex is fully consistent with the biochemical and NMR results.

DISCUSSION

Two monoclonal antibodies developed in our laboratory (mAb32 and mAb33) compete for binding to the C-terminal domain of HIV-1 IN (20), but affect its properties differently (14). Thus, these reagents provide valuable tools for probing the structure, dynamics, and function of this important enzyme. We previously mapped the binding of Fab32 to a specific region in the C-terminal domain using MALDI-TOF mass spectrometric analysis combined with time-limited proteolysis (22). Results from immunoblot studies in the present work confirmed that mAb33 also binds to residues in the C-terminal domain (amino acids 220–270) of HIV-1 IN. Although these two monoclonal antibodies bind to the same domain of IN, the affinities of mAb32 and Fab32 for the full-length HIV-1 IN protein are 100- and 10-fold lower than those of mAb33 and Fab33, respectively. The 10-fold difference in the binding affinities of mAb33 and its Fab fragment is consistent with the 10-fold difference in the ability of the two reagents to inhibit the catalytic activities of full-length IN. On the other hand, mAb32 and Fab32 have similar binding affinities, yet only the mAb shows a weak inhibition of IN catalysis, whereas the Fab fragment has no effect. SPR analyses show that Fab33 binding inhibits protein-DNA interaction, but Fab32 does not. Thus, these results indicate that the inhibitory activity of mAb32 may result solely from cross-linking due to its bivalency, whereas inhibition by mAb33 is likely due to direct interference with enzyme function.

Our previous studies showed that mAb17 and Fab17 binding to the N-terminal domain of HIV-1 IN can enhance the solubility of full-length HIV-1 IN in low ionic strength buffer (21). Here, we show that mAb32 and mAb33 and especially their Fab derivatives can also enhance IN protein solubility; neither catalytic core-specific Fab4 nor Fab19 displayed this activity.⁴ Such activity could result from masking of the hydrophobic residues in the epitope or from inhibition of oligomerization/aggregation by antibody binding. In either case, as the Fab33-IN complex is considerably more soluble than IN alone, it may prove to be a useful reagent for crystallization of IN.

Using limited proteolysis in conjunction with mass spectrometric analyses, residues in the HIV-1 IN C-terminal domain that are protected by binding of Fab32 were previously localized to two strands of the β -sheet, β_1 (Phe²²³, Arg²²⁴, Tyr²²⁶, and Arg²²⁸) and β_5 (Lys²⁶⁴, Lys²⁶⁶, and the side chain of Arg²⁶²) (22). However, efforts to map the epitope for Fab33 using the same method were unsuccessful because Fab33 binding renders the entire C-terminal domain (residues 220–270) resistant to proteolytic digestions (22). Thus, NMR was employed as an alternative method to identify residues that compose the epitope for Fab33. Although most of the residues in the C-terminal domain (39 of the 51 amino acids at positions 220–

⁴ J. Yi and A. M. Skalka, unpublished data.

270) are affected by addition of Fab33, a more detailed analysis of the backbone amide NH peak heights as a function of antibody concentration revealed substantial differences in the response to antibody binding among individual residues. Amino acids at or near the binding interface and interior residues are expected to show the most pronounced line broadening (and therefore decrease in peak height) as they are immobilized in the large Fab-IN complex. The steepest rate of this decrease is observed for some core residues, as well as a group of solvent-accessible residues that map to a contiguous area on the surface of the C-terminal domain, including Phe²²³, Arg²²⁴, and Tyr²²⁶ on β_1 ; Lys²⁴⁴ on β_2 ; and Ile²⁶⁷ and Ile²⁶⁸ on β_5 (Fig. 5). As these residues are largely immobilized in the complex with Fab33, they are likely to be located at or near the binding interface.

Comparison with residues protected by Fab32 (22) indicates that there is a partial overlap of amino acids in the C-terminal domain that are recognized by Fab32 and Fab33. For example, Phe²²³, Arg²²⁴, and Tyr²²⁶ on β_1 have been implicated in binding to both Fab32 and Fab33. This can explain the observed competition of the two antibodies for binding to the C-terminal domain. Although both antibodies interact with residues on β_5 , the two epitopes differ in detail (*i.e.* Fab32 binding protects Lys²⁶⁴ and Lys²⁶⁶, whereas Fab33 interacts with Ile²⁶⁷ and Ile²⁶⁸).

Two additional observations concerning the mobility of side chains are noteworthy. First, the majority of the side chains that are buried within the core of the C-terminal domain retain a higher degree of local mobility in the Fab33 complex compared with the residues assigned to the epitope. For example, the residues on β_1 facing the solvent (Phe²²³, Arg²²⁴, and Tyr²²⁶) are among the least mobile in the complex, whereas the adjacent core residues (Val²²⁵ and Tyr²²⁷) remain partially mobile upon complex formation (Fig. 4B). Second, the increased mobility of the backbone amides of Trp²⁴³, Val²⁵⁰, and Val²⁵⁹ could indicate either that Fab33 binding induces dissociation of the NMR-defined dimer interface or that it induces local conformational changes that affect residues in this region. Using mass spectrometry, SDS-PAGE, and size-exclusion chromatography, we could detect no effect of Fab33 binding on the monomer-dimer equilibrium of the C-terminal domain. Thus, we conclude that the mobility changes noted in interface residues by NMR are probably due to local conformational changes induced by binding of Fab33. This interpretation is consistent with the striking loss of protease sensitivity we previously observed with the Fab33-IN-(220–270) complex (22).

A number of C-terminal domain residues, including Ser²³⁰, Arg²³¹, Leu²³⁴, Lys²⁵⁸, Pro²⁶¹, Arg²⁶², and Lys²⁶⁴, have been implicated in DNA binding based on mutational analyses (16, 18, 31, 34). As illustrated in the molecular model of Fig. 9B, with the exception of Arg²⁶², there is no indication that these residues are contacted directly by Fab33. Recently, Gao *et al.* (35) reported that substitution of Arg²⁶² with Cys resulted in significant loss of IN activity *in vitro* and that this Cys residue could be cross-linked to a DNA substrate. Thus, the Arg²⁶² side chain may be important for DNA binding, and Fab33 contact with this residue could account for some of the Fab interference with DNA binding. We note, however, that this same residue is protected from proteolysis by Fab32 (22). As Fab32 does not prevent DNA binding to the C-terminal domain (Table I), it is possible either that these properties are not mutually exclusive or that contact with Arg²⁶² is insufficient to block DNA binding. An alternative explanation for interference by Fab33 with DNA binding is that the local conformational changes induced by the antibody cause sufficient rearrangement in IN-(220–270) to disrupt even distal DNA-binding determinants or to prevent

changes that occur upon DNA binding. Additional experiments will be required to test these hypotheses.

Although it has been known for some time that the C-terminal domain participates in IN protein-protein interaction (33, 34) and in sequence-independent DNA binding, its exact role in the integration reaction remains obscure. NMR studies show that the isolated C-terminal domain of HIV-1 IN forms a specific dimer in solution (16–18), whereas inspection of the x-ray crystal structure of a fragment that includes the catalytic core and C-terminal domains suggests that a variety of protein-protein interactions may be possible among the C-terminal domains in an active IN multimer (19). We speculate that the IN protein may have to assume different oligomeric configurations to function at specific stages in viral replication or to function in different parts of an asymmetric active complex (36) and that Fab33 binding may interfere with the protein-protein interactions that mediate these changes. Thus, further studies with Fab33 and full-length HIV-1 IN may provide additional insights into the role of the C-terminal domain in DNA binding and the conformational requirements for active multimerization. As Fab33 is a potent inhibitor of HIV-1 IN activity, residues composing its epitope may provide a novel target for the development of small molecule inhibitors. Various lines of evidence indicate that the Fab33 epitope in full-length HIV-1 IN is accessible *in vivo* (28, 37), implying a similar accessibility to possible therapeutic agents designed to target this site.

Acknowledgments—We thank Drs. G. M. Clore and A. M. Gronenborn for providing NMR assignments of the C-terminal integrase domain. NMR analyses were performed in the Fox Chase Spectroscopy Support Facility, and SPR and mass spectrometry were performed using instrumentation in the Fox Chase Fannie E. Ripple Biotechnology Facility with the assistance of Dr. S. H. Seeholzer. We are grateful to Patricia Roat for performing the ELISAs for Fig. 1C and George Merkel for the enzymatic assays for Fig. 2A. Dr. R. Wang (Mount Sinai School of Medicine) helped in the preparation of Fig. 6, and our Fox Chase colleagues Drs. G. D. Markham, S. H. Seeholzer, and R. A. Katz provided helpful comments on this work. We thank M. Estes for preparation of the manuscript.

REFERENCES

- Katz, R. A., and Skalka, A. M. (1994) *Annu. Rev. Biochem.* **63**, 133–173
- Andrake, M. D., and Skalka, A. M. (1996) *J. Mol. Chem.* **271**, 19633–19636
- Hindmarsh, P., and Leis, J. (1999) *Microbiol. Mol. Biol. Rev.* **63**, 836–843
- Cai, M., Zheng, R., Caffrey, M., Craigie, R., Clore, G. M., and Gronenborn, A. M. (1997) *Nat. Struct. Biol.* **4**, 567–577
- Eijkelenboom, A. P., van den Ent, F. M., Vos, A., Doreleijers, J. F., Hard, K., Tullius, T. D., Plasterk, R. H., Kaptein, R., and Boelens, R. (1997) *Curr. Biol.* **7**, 739–746
- Zheng, R., Jenkins, T. M., and Craigie, R. (1996) *Proc. Natl. Acad. Sci. U. S. A.* **93**, 13659–13664
- Lee, S. P., and Han, M. K. (1996) *Biochemistry* **35**, 3837–3844
- Lee, S. P., Xiao, J., Knutson, J. R., Lewis, M. S., and Han, M. K. (1997) *Biochemistry* **36**, 173–180
- Goldgur, Y., Dyda, F., Hickman, A. B., Jenkins, T. M., Craigie, R., and Davies, D. R. (1998) *Proc. Natl. Acad. Sci. U. S. A.* **95**, 9150–9154
- Maignan, S., Guilloteau, J. P., Zhou-Liu, Q., Clement-Mella, C., and Mikol, V. (1998) *J. Mol. Biol.* **282**, 359–368
- Bujacz, G., Jaskolski, M., Alexandratos, J., Wlodawer, A., Merkel, G., Katz, R. A., and Skalka, A. M. (1996) *Structure* **4**, 89–96
- Bujacz, G., Alexandratos, J., Wlodawer, A., Merkel, G., Andrake, M., Katz, R. A., and Skalka, A. M. (1997) *J. Biol. Chem.* **272**, 18161–18168
- Asante-Appiah, E., and Skalka, A. M. (1997) *J. Biol. Chem.* **272**, 16196–16205
- Asante-Appiah, E., Seeholzer, S. H., and Skalka, A. M. (1998) *J. Biol. Chem.* **273**, 35078–35087
- Yi, J., Asante-Appiah, E., and Skalka, A. M. (1999) *Biochemistry* **38**, 8458–8468
- Lodi, P. J., Ernst, J. A., Kuszewski, J., Hickman, A. B., Engelman, A., Craigie, R., Clore, G. M., and Gronenborn, A. M. (1995) *Biochemistry* **34**, 9826–9833
- Eijkelenboom, A. P., Puras-Lutzke, R. A., Boelens, R., Plasterk, R. H., Kaptein, R., and Hard, K. (1995) *Nat. Struct. Biol.* **2**, 807–810
- Eijkelenboom, A. P., Sprangers, R., Hard, K., Puras-Lutzke, R. A., Plasterk, R. H., Boelens, R., and Kaptein, R. (1999) *Proteins Struct. Funct. Genet.* **36**, 556–564
- Chen, J. C.-H., Krucinski, J., Miercke, L. J., Finer-Moore, J. S., Tang, A. H., Leavitt, A. D., and Stroud, R. M. (2000) *Proc. Natl. Acad. Sci. U. S. A.* **97**, 8233–8238
- Bizub-Bender, D., Kulkosky, J., and Skalka, A. M. (1994) *AIDS Res. Hum. Retroviruses* **10**, 1105–1115
- Yi, J., Arthur, J. W., Dunbrack, R. L., Jr., and Skalka, A. M. (2000) *J. Biol. Chem.* **275**, 38739–38748

22. Yi, J., and Skalka, A. M. (2000) *Biopolymers* **55**, 308–318
23. Kay, L. E., Keifer, P., and Saarine, T. (1992) *J. Am. Chem. Soc.* **114**, 10663–10665
24. Huang, X., Yang, X., Luft, B. J., and Koide, S. (1998) *J. Mol. Biol.* **281**, 61–67
25. Fraczekiewicz, R., and Braun, W. (1998) *J. Comp. Chem.* **19**, 319–333
26. Bower, M. J., Cohen, F. E., and Dunbrack, R. L., Jr. (1997) *J. Mol. Biol.* **267**, 1268–1282
27. Ritchie, D. W., and Kemp, G. J. L. (2000) *Proteins Struct. Funct. Genet.* **39**, 178–194
28. Levy-Mintz, P., Duan, L., Zhang, H., Hu, B., Dornadula, G., Zhu, M., Kulkosky, J., Bizub-Bender, D., Skalka, A. M., and Pomerantz, R. J. (1996) *J. Virol.* **70**, 8821–8832
29. Woerner, A. M., Klutch, M., Levin, J. G., and Marcus-Sekura, C. J. (1992) *AIDS Res. Hum. Retroviruses* **8**, 297–304
30. Vink, C., Oude Groeneger, A. M., and Plasterk, R. H. (1993) *Nucleic Acids Res.* **21**, 1419–1425
31. Puras-Lutzke, R. A., Vink, C., and Plasterk, R. H. (1994) *Nucleic Acids Res.* **22**, 4125–4131
32. Cheetham, J. C., Raleigh, D. P., Griest, R. E., Redfield, C., Dobson, C. M., and Rees, A. R. (1991) *Proc. Natl. Acad. Sci. U. S. A.* **88**, 7968–7972
33. Jenkins, T. M., Engelman, A., Ghirlando, R., and Craigie, R. (1996) *J. Biol. Chem.* **271**, 7712–7718
34. Puras-Lutzke, R. A., and Plasterk, R. H. (1998) *J. Virol.* **72**, 4841–4848
35. Gao, K., Butler, S. L., and Bushman, F. D. (2001) *EMBO J.* **20**, 3565–3576
36. Heuer, T. S., and Brown, P. O. (1998) *Biochemistry* **37**, 6667–6678
37. Visintin, M., Tse, E., Axelson, H., Rabbitts, T. H., and Cattaneo, A. (1999) *Proc. Natl. Acad. Sci. U. S. A.* **96**, 11723–11728
38. Kraulis, P. J. (1991) *J. Appl. Crystallogr.* **24**, 946–950
39. Merritt, E. A., and Bacon, D. J. (1997) *Methods Enzymol.* **277**, 505–524